

I. Bediaga,<sup>1,\*</sup> D.R. Boito,<sup>2,†</sup> G. Guerrer,<sup>1,‡</sup> F.S. Navarra,<sup>2,§</sup> and M. Nielsen<sup>2,¶</sup>
<sup>1</sup>*Centro Brasileiro de Pesquisas Físicas, Rua Xavier Sigaud 150, 22290-180 Rio de Janeiro, RJ, Brazil*
<sup>2</sup>*Instituto de Física, Universidade de São Paulo, C.P. 66318, 05389-970 São Paulo, SP, Brazil*

We evaluate the non-resonant decay amplitude of the process  $B^\pm \rightarrow K^\pm \pi^+ \pi^-$  using an approach based on final state hadronic interactions described in terms of meson exchanges. We conclude that this mechanism generates inhomogeneities in the Dalitz plot of the  $B$  decay.

PACS numbers: 13.25.Hw, 14.40.Nd, 12.38.Lg

## I. INTRODUCTION

The amplitude analysis of non-leptonic three body  $B$  decays became an important tool to determine the CKM phases [1, 2, 3], and also to observe CP-asymmetry. Using this method, the Belle and BaBar collaborations have recently [4, 5] extracted a fraction asymmetry for the channel  $B^\pm \rightarrow K^\pm \rho^0$ . With this kind of analysis one could also explore the asymmetry associated with the interference between two neighbour resonances decaying into the same three body final state.

The Dalitz plot analysis needs some *a priori* model, with all possible dynamical components and a correct functional form to be used to fit the Dalitz plot distribution. Arbitrary distribution functions can be used to get a good fit, but they have no physical meaning.

The non-resonant component which, in general, is spread all over the phase space, can mimic other dynamical components, through the interferences with the resonances present in the same phase space. This shadowing phenomenon was observed in charm three body decays in the E791 experiment [6, 7], where the overestimated contribution of the non-resonant amplitude replaced, in a wrong way, the contribution (and the very existence) of the scalar mesons  $\sigma$  and  $\kappa$ .

Belle has proposed, for the amplitude analysis of the process  $B^\pm \rightarrow K^\pm \pi^+ \pi^-$  [4], a parametrization for the non-resonant amplitude given by:

$$\mathcal{A}_{nr}(K^\pm \pi^\pm \pi^\mp) = a_1^{nr} e^{-\alpha s_{13}} e^{i\delta_1^{nr}} + a_2^{nr} e^{-\alpha s_{23}} e^{i\delta_2^{nr}}, \quad (1)$$

where  $a_1$ ,  $\delta_1$ ,  $a_2$  and  $\delta_2$  are the fit parameters and  $s_{13} \equiv M^2(K^\pm \pi^\mp)$  and  $s_{23} \equiv M^2(\pi^+ \pi^-)$  are the Dalitz variables. Originally the parametrization was also function of the variable  $s_{12} = M^2(K^\pm \pi^\pm)$ , but the term containing this variable turned out to give an insignificant contribution.

The function above could fit the data with an acceptable confidence level around 1%. Certainly this distribution was more useful for the Belle analysis than the usual

constant non-resonant distribution. However, it has to be employed with caution.

The use of an empirical parametrization, with a form without dynamical content, may hide the physical meaning of the Dalitz plot and, even worse, may yield inadequate parameters for the contribution of the resonance amplitudes and for the CP asymmetries. This is so because in the Dalitz distribution the parameters are highly correlated among themselves and also with the non-resonant amplitude. The parametrization (1) was proposed to describe non-uniformities in the non-resonant three-body decays. Data suggest the formation of a  $\pi^-$  with momentum predominantly smaller than the momentum of the  $K^+$  and  $\pi^+$  in the process  $B^+ \rightarrow K^+ \pi^+ \pi^-$ . How can we understand this?

In principle there are two different categories of dynamical processes contributing to the non-resonant structures in the Dalitz plot. One is a genuine three-body decay that is a consequence of the partonic structure of the weak decay [8, 9] and therefore will be called parton interaction, or PI. The other comes from final state hadron-hadron interactions [10, 11, 12, 13, 14, 15] and we shall call it FSI. In both approaches one is forced to make non-trivial calculation assumptions and the parameters and form factors are not well known. However as we are dealing with Dalitz distributions, the comparison of these different contributions with the experimental distributions might discriminate which dynamical mechanism is more realistic to describe data.

In Fig. 1 we show the diagrams relevant for the partonic description of this process. Figs. 1a and 1b show the direct and penguin contribution to the “current induced” processes. Figs. 1c), 1d) and 1e) show the direct (1c)) and and penguin (1d) and 1e)) contributions to the “transition” processes and and Figs. 1f) and 1g) show the direct and penguin “annihilation” processes.

Looking at diagrams 1a) to 1e) we can see that in the beginning both  $\bar{b}$  and  $u$  quarks can carry a large momentum. When they emit a  $W$  or a gluon, the bosons can also carry a large momentum and therefore, with the exception of the  $d$  and  $\bar{d}$  quarks (which come always from the vacuum and are soft) any of the quarks in the final state may carry a large momentum. This large momentum is then transferred to the final mesons. The final momentum distribution of the three mesons will be eventually non-uniform but there is no reason for producing

\*Electronic address: bediaga@cbpf.br

†Electronic address: dboito@if.usp.br

‡Electronic address: guerrer@cbpf.br

§Electronic address: navarra@if.usp.br

¶Electronic address: mnielsen@if.usp.br

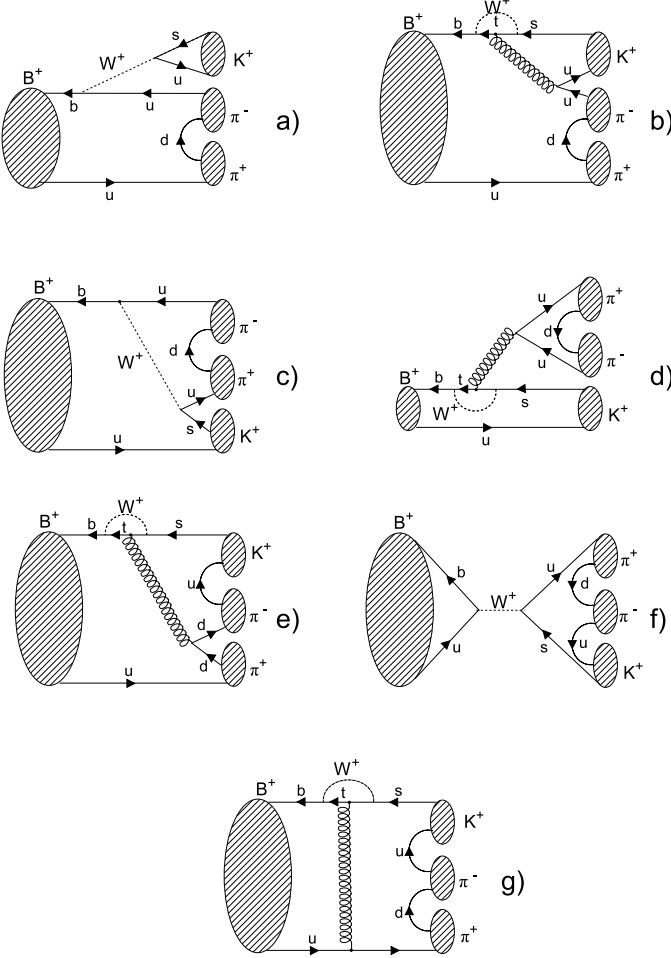


FIG. 1: Parton description of the weak decay  $B^+ \rightarrow K^+ \pi^+ \pi^-$ .

a softer  $\pi^-$ . The “entanglement” of the  $\bar{b}$ ,  $u$  and bosonic lines will distribute more or less democratically the initial high momenta. In sharp contrast to this situation are diagrams 1f) and 1g), where after the boson emission and absorption the high momenta are *only* with the  $u$  and  $\bar{s}$  quarks. In the middle of the diagrams we see the  $\pi^-$  made of  $u$  and  $d$  quarks pairs taken from the vacuum. This  $\pi^-$  will be comparatively softer than the negative pions of diagrams 1a) - 1e).

When the final three mesons are produced through final state interactions we can also understand the softer  $\pi^-$  in a very simple way: first the  $B^+$  decays into  $K^+$  and  $\pi^0$  and then these interact creating  $K^+$ ,  $\pi^+$  and  $\pi^-$ . The first two mesons carry the valence quarks of the more energetic intermediate  $K^+$  and  $\pi^0$  and therefore will have higher momenta. The  $\pi^-$  is produced with quarks taken from the vacuum and therefore is softer. This is illustrated in Fig.2. Thus the appearance of a comparatively soft  $\pi^-$  is nothing but the manifestation of the “leading

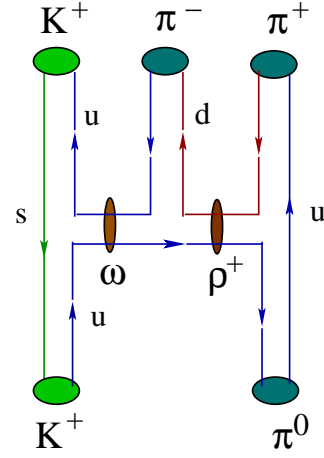


FIG. 2: Born diagram for  $K^+ \pi^0 \rightarrow K^+ \pi^+ \pi^-$  final state hadronic interaction.

particle effect”, so frequently observed in other processes in hadron physics.

To the best of our knowledge, this kind of process has been first observed in a Dalitz plot by the Aachen-Berlin-CERN Collaboration in the reaction  $\pi^- p \rightarrow \pi^+ \pi^0 n$  [16] and also in  $\pi^- p \rightarrow K^0 K^0 n$  [17]. Shortly after the experimental observation it was theoretically understood in [18]. In that paper it was explained in terms of double Regge graphs. This mechanism implies the production of a soft pion in the central region, responsible for a bump at the corner of the Dalitz plot, hence the name *cornering effect*.

The analysis performed in [19, 20], suggests that in the chiral limit approximation, i.e. when  $m_B^2 \gg m_K^2$ , diagram 1f) vanishes. It also suggests that the most important process is the one shown in Fig. 1g), which has a striking similarity with the diagram of Fig. 2. Both have the same final quark flow and final meson formation.

From the above qualitative discussion and from figures 1g) and 2 we conclude that in the decay  $B^+ \rightarrow K^+ \pi^+ \pi^-$  we expect to see a softer  $\pi^-$  which will yield a non-uniform Dalitz distribution. This effect comes both from the partonic weak decay and from final state interactions and has, in both cases, the same physical origin: valence quarks form hard mesons in the final state while softer mesons are produced from the vacuum. Neglecting the flavor change ( $\bar{b} \rightarrow \bar{s}$ ) in Fig. 1g), we can say that in both cases, PI and FSI, we have a leading particle effect.

In what follows we will implement these ideas in a more quantitative way. In view of the uncertainties in the partonic description, specially the use of the factorization hypothesis, we will develop here only the hadronic final state interaction approach, for which the relevant lagrangian densities and form factors are better known from a large body of phenomenological studies at low and intermediate energies. Therefore we shall suppose that the non-resonant three-body decay  $B^\pm \rightarrow K^\pm \pi^+ \pi^-$  proceeds through a hadronic scattering between two in-

intermediate mesons  $K^\pm$  and  $\pi^0$  in the two-body decay  $B^\pm \rightarrow K^\pm \pi^0$ .

## II. HADRONIC FINAL STATE INTERACTIONS

Hadronic final state interactions have a long story and follow two different approaches: Regge models and meson exchange models. The former have been considered in many works [10, 12] whereas the latter were discussed in [13, 14, 15]. Regge theory is formulated in the high energy limit and in it all the amplitudes respect unitarity constraints. The interactions are represented by reggeon exchanges, the Pomeron being usually the most important one. As one moves to the low energy region, secondary reggeons become important, additional assumptions have to be made and the theory loses predictive power. It is not clear when the energy starts to be “high” and Regge theory has been applied to energies of the order of a few GeV. Meson exchange models describe hadronic interactions fairly well at intermediate energies (a few hundreds MeV). They contain uncertainties associated with higher order diagrams, multiple exchange terms, coupling constants and the spatial extension of hadrons. These uncertainties are translated into form factors, which, in turn, can be either calculated (e.g. with QCD sum rules [21]) or simply parametrized and fitted to data. A positive aspect of meson exchange models is that one can use effective Lagrangians for them and so enforce chiral symmetry, which is known to be very important at intermediate energies. On the other hand, in this kind of model, the amplitudes are not unitary. The lack of unitarity is believed to become a serious problem at increasing energies. These considerations suggest that with increasing energies we should change the dynamical description, going from meson exchange to reggeon exchange, but is not clear *at which energy* this should be done. In this work we shall study final state interactions with meson dynamics.

In principle the  $B$  meson can decay into numerous hadronic two-body intermediate states which will subsequently decay into  $K^+ \pi^+ \pi^-$ . These states include:  $K^0 \pi^+$ ,  $K^+ \pi^0$ ,  $\eta' K^+$ ,  $\eta' K^{*+}$ ,  $\eta K^+$ ,  $\eta K^{*+}$ ,  $\omega K^+$ ,  $\omega K^{*+}$ ,  $a_0^+ K^0$ ,  $a_0^0 K^+$ ,  $K^{*0} \pi^+$ ,  $K^{*+} \pi^0$ ... These mesons can undergo a two-to-three reaction, exchanging virtual mesons and creating the  $\pi^-$ . This is illustrated in Fig. 2 for the  $K^+ \pi^0$  intermediate state, which we will use as working example. A more careful analysis reveals that some of the above mentioned two-body states can be excluded because their interactions yielding a  $K^+ \pi^+ \pi^-$  final state would violate  $G$  parity (this is the case of the  $K^0 \pi^+$  and  $a_0^+ K^0$ ). Some other states are much less abundant as two body decays. This is the case of the  $\omega K^+$  and  $\omega K^{*+}$  states, which branching fraction is one order of magnitude smaller than the  $K^+ \pi^0$  one. Other diagrams are suppressed by dual topological unitarity (DTU) [22]. Finally, some other states, inspite of being different, are expected to yield amplitudes which are qualitatively very

similar. This is, for example, the case of the states  $K^+ \pi^0$  and  $\eta' K^+$ . Replacing  $\pi^0$  by  $\eta'$  in Fig. 2 will lead to a similar diagram with the vertex  $\eta' \rho \pi$  instead of  $\pi \rho \pi$ . This will change the corresponding coupling constant and the form factor. The former is unable to distort the Dalitz plot and irrelevant for our discussion. In both vertices the form factor will suppress highly virtual internal  $\rho$  mesons. We therefore expect these two diagrams to give similar results. Even after a careful scrutiny and the elimination of suppressed diagrams and of “double counting”, there will remain a few diagrams to be considered. Here we shall work out in detail only the process depicted in Fig. 2. This will show schematically how the final state meson dynamics will lead to inhomogeneities in the Dalitz plot.

Before starting the evaluation of the Feynman diagram given in Fig. 2, one last remark is in order. In other FSI calculations, such as [14] the starting point is the  $B$  meson, which decays into two off-shell mesons, which, in turn exchange a third virtual meson. This process is described by a loop diagram, from which the absorptive part is considered. In our Fig. 2 this procedure would be equivalent to close the lower part of the diagram forming a loop with a virtual  $K^+$  and a virtual  $\pi^0$ . Here, for simplicity, we take them to be real. In this way we will give emphasis to the creation of the soft  $\pi^-$  and consequent Dalitz plot distortion. The loop integral will introduce some smearing in our result and presumably change the normalization. Since our purpose in this work is to discuss this process qualitatively, we postpone to the future a more general calculation, including effects of the kaon and pion off-shellness.

The effective Lagrangians relevant to the calculation can be constructed from a chiral Lagrangian [23]. They are:

$$\begin{aligned}\mathcal{L}_{\omega KK} &= ig_{\omega KK}(\bar{K}\partial_\mu K - \partial_\mu \bar{K}K)\omega^\mu, \\ \mathcal{L}_{\rho\pi\pi} &= g_{\rho\pi\pi}\vec{\rho}^\mu \cdot (\vec{\pi} \times \partial_\mu \vec{\pi}), \\ \mathcal{L}_{\rho\omega\pi} &= g_{\rho\omega\pi}\epsilon^{\alpha\beta\lambda\sigma}\partial_\beta\omega_\alpha\vec{\rho}_\lambda \cdot \partial_\sigma \vec{\pi}.\end{aligned}\quad (2)$$

With the above interaction Lagrangians, we can write the amplitude for the diagram in Fig. 2 as:

$$\mathcal{A} = \frac{4ig_{\omega KK}g_{\rho\pi\pi}g_{\rho\omega\pi}\epsilon^{\alpha\beta\lambda\sigma}p_{5\alpha}p_{2\beta}p_{1\lambda}p_{3\sigma}}{((p_1 - p_3)^2 - m_\omega^2)((p_5 - p_2)^2 - m_\rho^2)}, \quad (3)$$

where  $p_1$  and  $p_2$  denote the momenta of the  $K^+$  and  $\pi^0$  in the initial state;  $p_3$ ,  $p_4$  and  $p_5$  are those of the  $K^+$ ,  $\pi^-$  and  $\pi^+$  in the final state of the diagram in Fig. 2. It is important to notice that  $p_1 + p_2 = p_B$ , where  $p_B$  is the momentum of the  $B$  meson, since we are considering the final state interactions in the two-body decay  $B^+ \rightarrow K^+ \pi^0$ .

In order to take into account the effects of hadron internal structure we follow ref. [24] and introduce, in the amplitude, the form factor:

$$F(q_\omega, q_\rho) = \left( \frac{\Lambda^4}{\Lambda^4 + (q_\omega^2 - m_\omega^2)^2} \right) \left( \frac{\Lambda^4}{\Lambda^4 + (q_\rho^2 - m_\rho^2)^2} \right), \quad (4)$$

where  $q_\omega$  and  $q_p$  are the four momenta of the intermediate off-shell vector mesons, *i.e.*,  $q_\omega = p_1 - p_3$  and  $q_p = p_5 - p_2$  and  $\Lambda$  is a cut-off parameter taken to be  $\Lambda = 1$  GeV.

Parametrizing the amplitude of the weak decay  $B^+ \rightarrow K^+\pi^0$  through the weak decay coupling  $G_{BK\pi}$ , we can write the amplitude for the three-body decay,  $B^+ \rightarrow K^+\pi^+\pi^-$ , in terms of the  $K^+\pi^-$  ( $p_{K\pi} = p_3 + p_4$ ) and  $\pi^+\pi^-$  ( $p_{\pi\pi} = p_4 + p_5$ ) momenta as:

$$\mathcal{A}_{K\pi\pi} = \frac{-32i\Lambda^8 G_{BK\pi} g_{\omega KK} g_{\rho\pi\pi} g_{\rho\omega\pi}}{(q_1^2 - 4m_\omega^2)(\Lambda^4 + (q_1^2/4 - m_\omega^2)^2)} \times \frac{\epsilon^{\alpha\beta\lambda\sigma}(p_{\pi\pi})_\alpha p_{B\beta} P_\lambda (p_{K\pi})_\sigma}{(q_2^2 - 4m_\rho^2)(\Lambda^4 + (q_2^2/4 - m_\rho^2)^2)}, \quad (5)$$

where  $q_1 = P - p_B + 2p_{\pi\pi}$ ,  $q_2 = P + p_B - 2p_{K\pi}$  and  $P = p_1 - p_2$ . In terms of these momenta, the three-body decay rate is given by:

$$d\Gamma = \frac{|\mathcal{A}_{K\pi\pi}|^2}{2^4 \pi^5 m_B} \delta((p_{\pi\pi} + p_{K\pi} - p_B)^2 - m_\pi^2) \delta((p_B - p_{K\pi})^2 - m_\pi^2) \delta((p_B - p_{\pi\pi})^2 - m_K^2) d^4 p_{\pi\pi} d^4 p_{K\pi}. \quad (6)$$

Evaluating Eq. (6) and using the delta functions to perform some of the integrals, we finally write the decay rate in the standard form for the Dalitz plot:

$$\frac{d^2\Gamma}{ds_{13}ds_{23}} = \int \frac{|\mathcal{A}_{K\pi\pi}|^2}{2^8 \pi^4 m_B^2} d(\cos\theta_{K\pi}) d\phi_{\pi\pi}, \quad (7)$$

where, as in Eq. (1),  $s_{13} = p_{K\pi}^2$  and  $s_{23} = p_{\pi\pi}^2$ . In the rest frame of the  $B$  meson and due to the delta functions, in evaluating  $|\mathcal{A}_{K\pi\pi}|^2$  one has to use:

$$P^2 = 2m_\pi^2 + 2m_K^2 - m_B^2, \quad (8)$$

with

$$E_P = \frac{m_K^2 - m_\pi^2}{m_B} \text{ and } |\vec{P}| = \frac{\sqrt{\lambda(m_B^2, m_K^2, m_\pi^2)}}{m_B}, \quad (9)$$

where  $\lambda(x, y, z) = x^2 + y^2 + z^2 - 2xy - 2xz - 2yz$ . For the other momenta and scalar products we have:

$$q_1^2 = 2s_{23} - 2m_B^2 + 2m_K^2 + 4m_\pi^2 + 4P \cdot p_{\pi\pi}, \quad (10)$$

$$q_2^2 = 2s_{13} - 2m_B^2 + 2m_\pi^2 + 4m_K^2 - 4P \cdot p_{K\pi}, \quad (11)$$

$$P \cdot p_{K\pi} = E_P E_{K\pi} - |\vec{P}| |\vec{p}_{K\pi}| \cos\theta_{K\pi}, \quad (12)$$

$$P \cdot p_{\pi\pi} = E_P E_{\pi\pi} - |\vec{P}| |\vec{p}_{\pi\pi}| (\cos\theta_{K\pi} \cos\bar{\theta} + \sin\theta_{K\pi} \sin\bar{\theta} \cos\phi_{\pi\pi}), \quad (13)$$

$$\cos\bar{\theta} = \frac{(m_K^2 - m_\pi^2 - m_B^2 + s_{13} + s_{23} + \frac{(s_{13} - m_\pi^2)(s_{23} - m_K^2)}{m_B^2})}{4|\vec{p}_{K\pi}||\vec{p}_{\pi\pi}|}, \quad (14)$$

$$E_{K\pi} = \frac{m_B^2 + s_{13} - m_\pi^2}{2m_B}, \quad (15)$$

$$E_{\pi\pi} = \frac{m_B^2 + s_{23} - m_K^2}{2m_B}, \quad (16)$$

$$|\vec{p}_{\pi\pi}| = \frac{\sqrt{\lambda(m_B^2, s_{23}, m_K^2)}}{2m_B}, \quad (17)$$

$$|\vec{p}_{K\pi}| = \frac{\sqrt{\lambda(m_B^2, s_{13}, m_\pi^2)}}{2m_B}, \quad (18)$$

$$p_{\pi\pi} \cdot p_{K\pi} = \frac{m_B^2 - m_K^2}{2}. \quad (19)$$

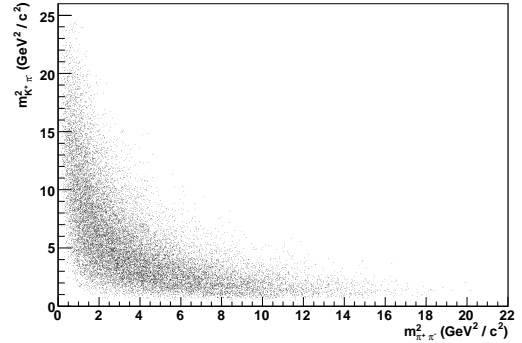


FIG. 3: The Dalitz plot for the non-resonant  $B^+ \rightarrow K^+\pi^+\pi^-$  decay.

For a given value of  $s_{13}$  ( $(m_\pi + m_K)^2 \leq s_{13} \leq (m_B - m_\pi)^2$ ), the range of  $s_{23}$  is determined by imposing  $-1 \leq \cos\bar{\theta} \leq 1$  and is given by [25]:

$$(s_{23})_{min} = (E_1^* + E_2^*)^2 - \left( \sqrt{E_1^{*2} - m_\pi^2} + \sqrt{E_2^{*2} - m_\pi^2} \right)^2$$

$$(s_{23})_{max} = (E_1^* + E_2^*)^2 - \left( \sqrt{E_1^{*2} - m_\pi^2} - \sqrt{E_2^{*2} - m_\pi^2} \right)^2$$

where

$$E_1^* = \frac{s_{13} - m_K^2 + m_\pi^2}{2p_{K\pi}},$$

$$E_2^* = \frac{m_B^2 - s_{13} - m_\pi^2}{2p_{K\pi}}.$$

Before presenting our numerical results we would like to emphasize that *we do not wish to reproduce the absolute normalization of the decay rate*. The only purpose of our calculation is to show that the meson exchange mechanism is able to produce distortions in the Dalitz plot of the  $B^+ \rightarrow K^+\pi^+\pi^-$  decay.

In Fig. 3 we show the Dalitz plot of a Monte Carlo simulation of Eq. (7). The distribution shown in the figure is consistent with the parametrization in Eq.(1) but it goes to zero near the threshold. This result gives support to the expectation presented in section II: the  $K^+$  and  $\pi^+$  carry the valence quarks from the intermediate  $K^+$  and  $\pi^0$  and are therefore hard, while the  $\pi^-$  is created from the vacuum and is therefore softer.

The Dalitz distribution of Fig. 3 can be parametrized as

$$|\mathcal{A}_{nr}(K^+\pi^-\pi^+)|^2 \propto \sqrt{s_{23}s_{13}} f_1(s_{23}) f_2(s_{13}) e^{-D s_{23}^2 s_{13}^2} \quad (20)$$

where

$$f_i(x) = \frac{1}{1 + e^{[c_i(x-p_i)]}} \quad (21)$$

with  $D = 1.3232 \times 10^{-3} \text{ GeV}^{-8}$ ,  $c_1 = 0.65 \text{ GeV}^{-2}$ ,  $p_1 = 18 \text{ GeV}^2$ ,  $c_2 = 0.55 \text{ GeV}^{-2}$  and  $p_2 = 15 \text{ GeV}^2$ .

The meson exchange mechanism considered above could play the same role in the  $D^+ \rightarrow K^-\pi^+\pi^+$  three-body decay, where one does not see any inhomogeneity in the non-resonant amplitude. In the case of the  $D^+$ , the three-body decay could proceed through final state interactions between the  $K_s$  and  $\pi^+$  mesons in the two-body decay  $D^+ \rightarrow K_s\pi^+$ . In Fig. 4 we show the Feynman diagram for the  $D^+ \rightarrow K^-\pi^+\pi^+$  decay through the  $K_s\pi^+$  interaction. We see that there are no mesons that could be exchanged satisfying all the conservation laws required by strong interactions. This means that the diagram does not exist and the three-body decay  $D^+ \rightarrow K^-\pi^+\pi^+$  does not proceed through final state interactions. A similar situation occurs in the three-body decay  $B^+ \rightarrow D^-\pi^+\pi^+$ , since there is no possible meson exchange that would lead the two mesons  $\bar{D}^0$  and  $\pi^+$  in the two-body decay  $B^+ \rightarrow \bar{D}^0\pi^+$  into the final three mesons:  $D^-\pi^+\pi^+$ . On the other hand, the three-body decay  $B^0 \rightarrow K^+K^-\pi^0$  can proceed through the two-body decay  $B^0 \rightarrow K^+\pi^-$ , followed by final state interactions between  $K^+$  and  $\pi^-$ , as can be seen by the Feynman diagrams in Fig. 5.

Therefore, in the case of the three-body decay  $B^0 \rightarrow K^+K^-\pi^0$ , one expects some inhomogeneity in the non-resonant amplitude, consistent with a hard  $K^+$ , a hard  $K^0$  and a softer  $K^-$ . This effect was not included in the data analysis performed by the BaBar Collaboration in ref. [29], where a homogeneous parametrization for the non-resonant component was used.

To close this section we would like to comment the Belle results on baryonic three body decays. In this context the FSI approach was first used in [30] to study rare baryonic  $B$  decays.

The study of the decays  $B^+ \rightarrow p\bar{p}K^+$ ,  $B^+ \rightarrow p\bar{p}\pi^+$  [31] revealed a low mass enhancement of the system  $p\bar{p}$ . However this enhancement in the low mass (close to the threshold) baryon-antibaryon system was not seen in the decays  $B \rightarrow p\bar{p}J/\psi$  and  $B^- \rightarrow \Lambda\bar{\Lambda}J/\psi$  [32]. In terms of FSI we can very easily understand these

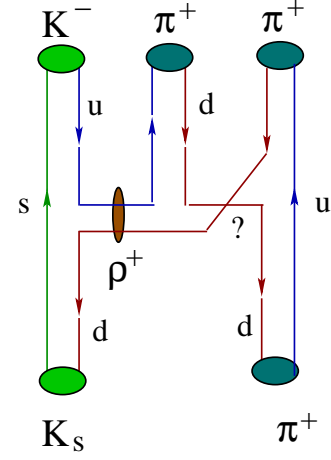


FIG. 4: Born diagram for  $K_s\pi^+ \rightarrow K^-\pi^+\pi^+$  final state hadronic interaction.

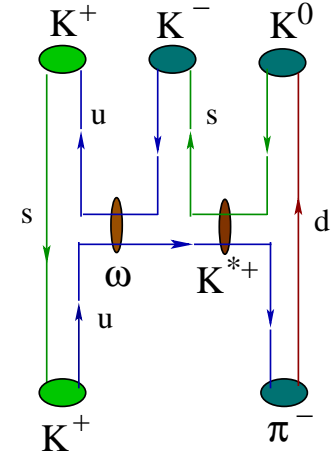


FIG. 5: Born diagram for  $K^+\pi^- \rightarrow K^+K^-\pi^0$  final state hadronic interaction.

results. The mass of the baryon-antibaryon system is low because the  $\bar{p}$  is soft. In the case of light meson production we have the following sequence of decays:  $B^+ \rightarrow K^+\pi^0 \rightarrow K^+p\bar{p}$ . The intermediate pion splits into a proton and an antiproton and the latter interacts with the kaon exchanging a  $\rho$  or an  $\omega$ . The emerging  $\bar{p}$  has all the antiquarks coming from the vacuum and will therefore carry low momentum. In the case of  $J/\psi$  production the  $B$  goes first to an intermediate state with  $J/\psi$ , such as, for example,  $J/\psi\pi^0$ . The pion could then split into  $p$  and  $\bar{p}$  but now the subsequent elastic interaction between the  $J/\psi$  and the  $\bar{p}$  is OZI suppressed, since the two mesons have no quarks in common. Therefore, in this case there is no soft  $\bar{p}$  from FSI and no low mass enhancement in the  $p\bar{p}$  system. This same problem has been addressed in [10] where a similar conclusion was obtained.

### III. CONCLUDING REMARKS

We hope to have made clear that, for experimental purposes, it is highly desirable to have a parametrization for the amplitude of non-resonant three body decays. This parametrization should have a physical basis and should be derived from theory. The already existing parametrization given in Eq. (1) is not satisfactory from this point of view. In order to improve it we have considered one possible mechanism responsible for inhomogeneities in the Dalitz plot, which we have called final state interactions (FSI). We have sketched calculations

of the Dalitz distributions with this mechanism. These calculations can certainly be improved, but already at this stage they can teach us how to obtain distortions in the non-resonant three body decays. FSI trace back the observed Dalitz distributions to a manifestation of the leading particle effect.

### Acknowledgements

This work has been partly supported by FAPESP and CNPq.

- 
- [1] A.E. Snyder and H. Quinn, Phys. Rev. D 48 (1993) 2139.
  - [2] I. Bediaga, G. Guerrer and J.M. de Miranda, hep-ph/0608268 and hep-ph/0703131.
  - [3] M. Ciuchini, M. Pierini, L. Silvestrini, Phys. Lett. B 645 (2007) 201.
  - [4] Belle Collaboration, A. Garmash *et al.*, Phys. Rev. D 71 (2005) 092003; K. Abe *et al.*, hep-ex/0509001.
  - [5] BaBar Collaboration, B. Aubert *et al.*, Phys. Rev. D 72 (2005) 072003, Erratum-ibid. D 74 (2006) 099903; and hep-ex/0507004.
  - [6] E.M. Aitala *et al.*, Phys. Rev. Lett. 86 (2001) 770.
  - [7] E.M. Aitala *et al.*, Phys. Rev. Lett. 89 (2002) 121801.
  - [8] I. Bediaga, C. Göbel and R. Méndez-Galain, Phys. Rev. Lett. 78 (1997) 22.
  - [9] I. Bediaga, C. Göbel and R. Méndez-Galain, Phys. Rev. D 56 (1997) 4268.
  - [10] V. Laporta, Int. J. Mod. Phys. A 22 (2007) 5401.
  - [11] A. Deandrea, M. Ladisa, V. Laporta, G. Nardulli and P. Santorelli, Int. J. Mod. Phys. A 21 (2006) 4425; H. Y. Cheng, Int. J. Mod. Phys. A 21 (2006) 650.
  - [12] J. F. Donoghue, E. Golowich, A. A. Petrov and J. M. Soares, Phys. Rev. Lett. 77 (1996) 2178.
  - [13] for a recent comprehensive review see: H. Y. Cheng, C. K. Chua and A. Soni, Phys. Rev. D 71 (2005) 014030.
  - [14] X. Liu, B. Zhang, L. L. Shen and S. L. Zhu, Phys. Rev. D 75 (2007) 074017; X. Liu, B. Zhang and S. L. Zhu, Phys. Lett. B 645 (2007) 185; X. Liu and X. Q. Li, arXiv:0707.0919 [hep-ph].
  - [15] N. Isgur, K. Maltman, I. Weinstein and T. Barnes, Phys. Rev. Lett. 64 (1990) 161; H. Lipkin and B.S. Zou, Phys. Rev. D 53 (1996) 6693; P. Geiger and N. Isgur, Phys. Rev. Lett. 67 (1991) 1066; X.Q. Li, D.V. Bugg and B.S. Zou, Phys. Rev. D 55 (1997) 1421.
  - [16] Aachen-Berlin-CERN Collaboration, Phys. Lett. 18 (1965) 351.
  - [17] W. Beusch *et al.*, International Conference on High-Energy Physics, Berkeley (1966).
  - [18] C. Hong-Mo, K. Kajantie and G. Ranft, Il Nuovo Cimento IL A (1967) 157.
  - [19] H.-Y. Cheng, C.-K. Chua and A. Soni, Phys. Rev. D 76 (2007) 094006.
  - [20] H.-Y. Cheng and K.-C. Yang, Phys. Rev. D 66 (2002) 054015.
  - [21] F. S. Navarra, M. Nielsen and M. E. Bracco, Phys. Rev. D 65 (2002) 037502; R. D. Matheus, F. S. Navarra, M. Nielsen and R. Rodrigues da Silva, Phys. Lett. B 541 (2002) 265.
  - [22] G.F. Chew and C. Rosenzweig, Phys. Rep. 41 (1978) 263.
  - [23] W. Liu, C.M. Ko and L.W. Chen, Nucl. Phys. A 765 (2006) 401.
  - [24] W. Liu and C.M. Ko, Phys. Rev. C 69 (2004) 045204.
  - [25] Particle Data Group, Y.M. Yao *et al.*, J. Phys. G 33 (2006) 1.
  - [26] C.L.Y. Lee, M. Lu and M.B. Wise, Phys. Rev. D 46 (2002) 054015.
  - [27] J.H. Kühn and E. Mirkes, Z. Phys. C 56 (1992) 661.
  - [28] M. Wirbel, B. Stech and M. Bauer, Z. Phys. C 29 (1985) 637.
  - [29] B. Aubert *et al.* (BaBar Collaboration), hep-ex/0607112.
  - [30] W. S. Hou and A. Soni, Phys. Rev. Lett. 86 (2001) 4247; arXiv:hep-ph/0008079.
  - [31] M. Z. Wang *et al.*, Phys. Lett. B 617 (2005) 141; J. T. Wei *et al.* [BELLE Collaboration], Phys. Lett. B 659 (2008) 80.
  - [32] Q. L. Xie *et al.* [Belle Collaboration], Phys. Rev. D 72 (2005) 051105.